

1-[Ferrocenyl(hydroxy)methyl]-1,7-dicarba-*closo*-dodecaborane: Synthesis and X-ray crystal structure

Jerry Fields,⁽¹⁾ Xiang Ouyang,⁽²⁾ Steven R. Herron,⁽³⁾ Katherine A. Kantardjieff,⁽²⁾ Ali Jabalameli,⁽¹⁾ and Frank A. Gomez^{(1)*}

Received October 21, 2005; accepted September 5, 2006
Published Online December 1, 2006

The synthesis and molecular structure of the novel 1-[ferrocenyl(hydroxy)methyl]-1,7-dicarba-*closo*-dodecaborane (**1**) is described. Compound **1** was synthesized from reaction of *m*-carborane and ferrocene carboxaldehyde using *n*-butyllithium (*n*-BuLi) or tetrabutylammonium fluoride (TBAF) in THF in 45% and 36% yield, respectively. Compound **1** consists of a ferrocene molecule tethered to *m*-carborane through a methylhydroxy bridge. The crystal structure of **1** was determined by single crystal X-ray diffraction analysis. Crystal data: **1** [Fe(C₅H₅)(C₅H₄-CH₂O-1,7-C₂B₁₀H₁₂)], formula weight = 359.17, crystallized in orthorhombic system, space group *Pna2*₁ with *a* = 19.698(4) Å, *b* = 10.709(2) Å, *c* = 8.520(2) Å, and *V* = 1797.3(7) Å³ and *Z* = 4. Refined to *R*₁ = 0.043 for 4124 observed reflections with *I*/*σ* > 2*σ*(*I*). The compound was crystallized as racemic twins in a ratio of 73(2)/27(2). The unsubstituted Cp ring was disordered and modeled as two conformations in a 53(3)/47(3) ratio. Intermolecular hydrogen bonding was observed from the hydrogen of the *meta*-carbon on the carborane cluster towards the hydroxyl oxygen.

KEY WORDS: Ferrocene; carborane; meta-carborane; nucleophilic substitution; crystal structure.

Introduction

Carboranyl species have been shown to be versatile ligands with an array of applications including boron neutron capture therapy (BNCT) and as polymeric conductors. The icosahedral

carboranes 1,2-, 1,7-, and 1,12-dicarba-*closo*-dodecaboranes (Fig. 1) in particular, have been widely used, due to their diverse properties that can be tuned via synthetic approaches, and the fascinating structures that result from their modification. Our recent focus has been in developing simple and versatile synthetic routes to carborane and ferrocene-containing species for use as starting synthons to boron-containing polymers.

The following report details the X-ray crystal structure and analysis of the novel metallocarborane complex, 1-[ferrocenyl(hydroxy)methyl]-1,7-dicarba-*closo*-dodecaborane (**1**). The synthesis of **1**, from *m*-carborane, follows that of the corresponding 1-[ferrocenyl(hydroxy)methyl]-1,

⁽¹⁾ Department of Chemistry and Biochemistry, California State University, Los Angeles, 5151, State University Drive, Los Angeles, CA 90032-8202, USA.

⁽²⁾ Department of Chemistry and Biochemistry, California State University, Fullerton 800, N. State College Boulevard, Fullerton, CA 92834-6866, USA.

⁽³⁾ Present Address: Department of Chemistry and Biochemistry, Brigham Young University, Provo, UT 84602, USA.

* To whom correspondence should be addressed; e-mail: fgomez2@calstatela.edu.

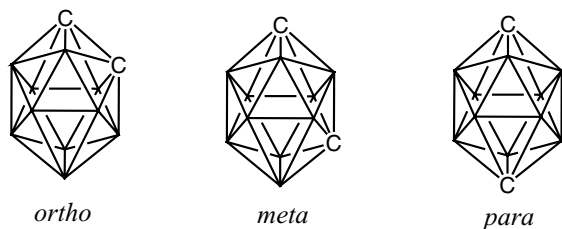


Fig. 1. Vertices with carbon atoms are indicated all others correspond to boron atoms. Single hydrogen atoms attached to each vertex are not shown.

2-dicarba-*closo*-dodecaborane molecule (**2**), (using *o*-carborane as starting material), previously reported by our laboratories.¹ The difference among the two carborane isomers is the location of the two carbon atoms in the icosahedral structure.

In our earlier work, we attempted to prepare a di-substituted carborane from *o*-carborane and ferrocenecarboxaldehyde, but only the mono-substituted product **2** was observed. The reason di-substitution did not occur with *o*-carborane may be attributed to steric hindrance between substituents as a result of the carborane carbon atoms being adjacent to one another. The proximity of the carbon atoms in *m*-carborane, (separated by a boron atom), should reduce steric effects, thereby allowing for the formation of a di-substituted product.

Relatively few substituted *m*-carborane complexes have been synthesized in comparison to *o*-carborane. The fact that *m*-carborane is used to a lesser extent may be attributed in part to the lower electronegativity of its carbon atoms, and stability of products formed.² Activation of carborane carbon atoms for substitution reactions can be achieved by using *n*-butyllithium (*n*-BuLi) to form lithiocarborane (where the proton on the carbon atom is substituted by lithium), or by forming the carborane anion using a relatively mild base such as tetrabutylammonium fluoride (TBAF) to remove a proton from carbon. The use of TBAF is of particular importance where substituents may be sensitive to highly basic conditions.³

A major benefit to synthesizing mono-substituted carborane derivatives from carborane

itself, rather than reaction between decaborane ($B_{10}H_{14}$) and a substituted acetylene, is the greater variety of substituted species that are possible.⁴ Among the many types of functionalized carborane complexes possible are a variety of transition metal derivatives.^{5,6} In particular, the attachment of transition metal complexes such as ferrocene to carborane offers a variety of potential applications including those in the fields of medical research, microelectronics and electro-optics.⁷⁻⁹ The electronic properties of carborane and ferrocene make them particularly well-suited for microelectronic applications, because carboranes are electron-withdrawing and the aromatic cyclopentane rings in ferrocene lower the oxidative potential of iron.

Herein, we describe the synthesis and molecular structure of 1-[ferrocenyl(hydroxy)methyl]-1,7-dicarba-*closo*-dodecaborane (**1**). This compound is further proof of the unique reactive properties of carboranyl species and their potential use in various applications.

Experimental

Synthesis

The experimental methods outlined here are based on those used in the synthesis of **2**. Reactions were conducted under dry conditions in a glovebox (N_2), at room temperature. Separate solutions, 0.1 M, of *m*-carborane ($1,7-C_2B_{10}H_{12}$) and ferrocenecarboxaldehyde ($Fe(C_5H_5)(C_5H_4CHO)$) were made in 10-mL of dry THF. A 1:1 stoichiometric equivalent of BuLi (2.5 M in hexanes), or TBAF (1.0 M in THF), was added to the *m*-carborane solution. When TBAF was used the solution of ferrocenecarboxaldehyde was added simultaneously to the *m*-carborane reaction mixture and stirred continuously for 30 min. When BuLi was used, the *m*-carborane reaction mixture was stirred for 30 min prior to ferrocenecarboxaldehyde addition and mixed for 24 h. Following quenching with H_2O , solutions were extracted with ether, washed, dried, and concentrated

under vacuum. The mono-substituted *m*-carborane ferrocenecarbinol product **1**, was purified by silica gel column chromatography using chloroform/hexanes, 1:2, and was obtained in 36% yield when TBAF was used, and 45% yield when BuLi was used: mp 110–113°C.

Infrared spectra

Infrared spectra were recorded on a Nicolet-Avatar 320 FT-IR using a KBr pellet. IR (Nujol, cm^{-1}): 3100 (w), 2600 (s), 2350 (s), 1150 (s).

NMR spectra

The proton decoupled ^{13}C NMR experiments were carried out on a Bruker DRX 400 NMR spectrometer operating at 9.4 T. All spectra were recorded using a 5 mm QNP probe with the following experimental conditions: base frequency of 100.625 MHz, block size of 32k, flip angle of 75°, recycling delay time of 4 s (5 times T1) and sweep width of 22000 Hz (quadrature phase detection on). Chemical shifts were measured in parts per million with reference to the solvent (CDCl_3) peak at 77.0 ppm. The ^1H and ^{11}B NMR spectra were recorded on a Bruker AC300 operating at 7.05 Tesla equipped with 5 mm BB probe. For ^1H NMR, the following experimental conditions were applied: base frequency of 300.136 MHz, block size of 32k, flip angle of 75°, recycling delay time of 3 s (5 times T1) and sweep width of 3000 Hz (quadrature phase detection on). Chemical shifts were measured in parts per million with reference to the solvent (CDCl_3) peak at 7.24 ppm. For proton decoupled ^{11}B NMR, following experimental conditions were used: base frequency of 96.290 MHz, block size of 16k, flip angle of 75°, recycling delay time of 4 s (5 times T1) and sweep width of 2000 Hz (quadrature phase detection on). Chemical shifts were measured in parts per million with reference to the external reference boric acid peak at 0.7 ppm. ^1H NMR (CDCl_3 , ppm): 4.8–4.0 (9 H, Cp-H), 3.9–1.0 (11 H, Cb-H). ^{11}B NMR (CDCl_3 , ppm),

Ref., boric acid: –25 (d, 1 B), –28 (d, 1 B), –33 (d, 2 B), –35 (d, 2 B), –37 (d, 2 B), –39 (d, 2 B). ^{13}C NMR (CDCl_3 , ppm): 91 (t, 1 C), 72 (t, 2 C), 70 (q, 1 C), 69 (t, 5 C), 64 (d, 1 C), 54 (t, 2 C), 30 (t, 1 C).

Mass spectra

Samples were analyzed on an Applied Biosystems Voyager System 4397 mass spectrometer using 2,5 dihydroxybenzoic acid as matrix. Reflector mode mass spectra were accumulated for 50 laser shots per sample spot with a nitrogen laser (337 nm, 4 ns pulses of 180 μJ), and a positive ion TOF detection was performed using an accelerating voltage of 20 kV. A blank spectrum to identify the matrix peaks were also carried out. The sample was prepared with a concentration of 100 pmol/ μl with the matrix of 10 mg/ml in acetonitrile solvent. MALDI-TOF MS: $m/z = 357.7$, theoretical mass = 358.3 g/mol.

Crystallography

Solid crystals of the product title compound were obtained from the slow evaporation of a chloroform/hexanes (1:1) solution to give orange diamond shaped crystals. A single crystal of compound **1** of appropriate size was mounted on a Bruker AXS CCD platform diffractometer with Mo $K\alpha$ ($\lambda = 0.71073 \text{ \AA}$) radiation at –30°C. An entire hemisphere of data was collected in multiple runs mode with Scan width 0.3° in ω , with three sets of 606 frames at ϕ at 0, 120 and 240° and a fourth set of 50 redundant frames at ϕ at 0 to check for crystal decay. A total of 1868 frames were collected at 30 s per frame. Detector-to-sample distance was 4.98 cm. Data collection and cell parameter determination were performed with SMART 5.4.¹² Data collection and cell parameter determination were performed with SMART 5.4, and data integration and reduction were performed with SAINT 6.2,¹³ both from Bruker AXS. Laue crystal symmetry restraints were used during data integration. Final cell parameters were obtained by refining

the *xyz* centroid of 6384 strong reflections with $I/\sigma > 5$ to yield $a = 19.698(4)$ Å, $b = 10.709(2)$ Å, $c = 8.520(2)$ Å, and $V = 1797.3(7)$ Å³. The intensities were corrected for Lorentz and polarization effects and for absorption with SADABS.¹⁴ Friedel pairs were not merged. The correction led to a transmission parameter between 1 and 0.80. Of the 14843 reflections collected, 4124 are unique ($R_{\text{int}} = 0.0442$). A summary of crystallographic data is given in Table 1. Complete crystallographic data, as a CIF file, have been deposited with the Cambridge Crystallographic Data Centre (CCDC No 285034). A copy of this file can be obtained free of charge from: The Director, CCDC, 12 Union Road, Cambridge CB2 1EZ, U.K. (e-mail: deposit@ccdc.cam.ac.uk).

The structure of the title compound was solved by Direct Methods and refined in space group *Pna2*₁ using the SHELXTL 5.10 package.¹³ All nonhydrogen atoms were refined anisotropically with full-matrix least-squares on F^2 . Hydrogen atoms were assigned to their ideal positions, and refined isotropically. The hydroxyl H atom was located by difference map. The idealized O–H bond length was used, and the hydroxyl hydrogen was allowed to rotate around the O–C bond to maximize the electron density. Racemic twinning was suggested during refinement, and a batch number was used to refine the twinning ratio to 73(2)/27(2). The unsubstituted Cp ring was disordered and modeled as two approximate half/half conformations, staggered (*A*) and eclipsed (*B*), which refined to a 53(3)/47(3) ratio. A five-fold symmetry restraint was applied to the Cp model and allowed to expand or shrink during refinement. The largest peak and hole of 0.30 and -0.29 electron Å⁻³ on the final difference map are both near Fe1.

Results

The carborane cage in **1** is a highly distorted icosahedron. B–C bond lengths in the cage are between 1.679(4) Å and 1.726(4) Å, with the shortest B–C bond between B8–C13, in which the B

Table 1. Crystallographic Data for [Fe(C₅H₅)(C₅H₄-CH(OH)-1,7-C₂B₁₀H₁₂)] (**1**)

Empirical formula	C ₁₃ H ₂₂ B ₁₀ FeO
CCDC deposition #	285034
Formula weight	358.26
Temperature (K)	243(2)
Wavelength (Å)	0.71073
Crystal dimension (mm ³)	0.5 × 0.42 × 0.4
Crystal system	Orthorhombic
Space group	<i>Pna2</i> ₁
Unit cell dimensions	
<i>a</i> (Å)	19.698(4)
<i>b</i> (Å)	10.709(2)
<i>c</i> (Å)	8.520(2)
<i>V</i> (Å ³)	1797.3(7)
<i>Z</i>	4
Density (calculated) (g/cm ³)	1.324
Absorption coefficient (mm ⁻¹)	0.835
Transmission factors, $T_{\text{min}}/T_{\text{max}}$	0.68/0.73
Diffractometer	Bruker Smart 1K CCD
Scan	ϕ and ω
θ range for data collection (°)	2.07 to 28.33
Reflections measured	14843
Independent observed reflections	4124 [$R_{\text{int}} = 0.0442$]
Independent reflections [$I > 2\sigma(I)$]	3252
Completeness to $\theta = 27.50^\circ$	99.6 %
Data/restraints/parameters	4124/61/281
Goodness-of-fit on F^2	1.032
Final <i>R</i> indices [$I > 2\sigma(I)$]	$R_1 = 0.0433$, $wR_2 = 0.0905$
<i>R</i> indices (all data)	$R_1 = 0.0624$, $wR_2 = 0.0968$
Absolute structure parameter	0.27(2)
Extinction coefficient	0.0024(4)
Largest diff. peak and hole	0.297 and -0.294 e.Å ⁻³ (both are near Fe1)
Racemic twinning ratio	73(2)/27(2)

Note. $R_1 = \sum ||F_o| - |F_c|| / \sum |F_o|$, $wR_2 = \{\sum [w(F_o^2 - F_c^2)^2] / \sum [w(F_o^2)^2]\}^{1/2}$, $w = 1/[\sigma^2(F_o^2) + (aP)^2 + bP]$

atom bridges two C's. Selected bond lengths are shown in Table 2. The smallest <C–B–C angle is the <C7–B12–C13 bond angle of 101.7(2)°. B–B bond lengths are in the range of 1.751(6) Å to 1.791(5) Å. An intermolecular hydrogen bond from the *meta*-carbon on the cage towards the hydroxyl oxygen is observed, with a C13...O1 donor to acceptor distance of 3.229(3) Å.

The hydroxyl H atom, pointing towards the unsubstituted Cp ring, was located by difference map. This hydrogen is not involved in a traditional hydrogen bond, but rather points to the

Table 2. Selected Bond Lengths (Å) and Angles (°) for **1**

A–B	Å	A–B	Å
Fe1–C3	2.038(4)	C7–B8	1.703(4)
Fe1–C2	2.041(3)	C7–B9	1.714(5)
Fe1–C4	2.049(4)	C7–B10	1.726(4)
Fe1–C6	2.052(3)	C7–B11	1.724(4)
Fe1–C5	2.052(3)	B8–C13	1.679(4)
O1–C1	1.408(3)	B12–C13	1.706(4)
C1–C2	1.502(3)	C13–B14	1.706(5)
C1–C7	1.560(4)	C13–B17	1.707(5)
C2–C3	1.421(5)	C13–B18	1.712(5)
C2–C6	1.437(4)	B14–B18	1.755(6)
C3–C4	1.421(5)	B15–B18	1.776(6)
C4–C5	1.422(6)	B16–B18	1.791(5)
C5–C6	1.411(4)	B17–B18	1.790(6)
C7–B12	1.694(4)	B10–B16	1.751(6)
<(A–B–C)	(°)	<(A–B–C)	(°)
O1–C1–C2	112.3(3)	C7–B8–C13	102.5(2)
O1–C1–C7	107.8(2)	C7–B9–B15	105.6(3)
C2–C1–C7	112.2(2)	C7–B10–B16	105.9(3)
C3–C2–C6	107.9(3)	C7–B11–B17	103.9(2)
C3–C2–C1	126.9(3)	C7–B12–C13	101.7(2)
C6–C2–C1	125.2(3)	B8–C13–B18	114.0(2)
C2–C3–C4	107.9(3)	B9–B14–B18	108.1(2)
C5–C4–C3	108.2(3)	B11–B16–B18	108.0(2)
C6–C5–C4	108.4(3)	B12–B17–B18	108.0(2)
C5–C6–C2	107.7(3)	B10–B15–B18	107.6(3)
C1–C7–B12	120.0(2)	C13–B18–B16	104.3(3)
C1–C7–B8	119.5(2)	B14–B18–B17	108.0(2)
C1–C7–B9	116.7(2)	C13–B18–B15	104.8(3)
C1–C7–B10	117.3(2)	B14–B18–B16	108.1(3)
C1–C7–B11	118.6(2)	B15–B18–B17	107.5(3)
D–H...A	D–H (Å)	D...A (Å)	<(DHA) (°)
C13A–H13...O1	1.11	3.229(3)	138.5
O1–H1a...Fe1	0.83	3.533(2)	119.5
O1–H1a...C19	0.83	3.620(17)	158.6
O1–H1a...C19b	0.83	3.558(16)	150.3

Fe of the ferrocene, with an OH...M distance of 3.05 Å. The hydroxyl H atom also points towards the unsubstituted Cp ring, with OH...C distance of 2.81–2.83 Å. The distance from the Fe to the least-square plane of the substituted Cp ring is 1.650(2) Å, and the distance from the Fe to the least-square plane of the disordered unsubstituted Cp rings is 1.686(7) Å, with an average C–C bond length of 1.37(1) Å for conformation *A*. The Fe–Cp distance is 1.660(9) Å with an average C–C bond length of 1.40(1) Å for conformation *B*.

Discussion

The refined occupancy ratio for the two Cp ring conformations are 53(3)/47(3), with the occupancy of the staggered conformation (*A*) slightly higher than the eclipsed conformation (*B*). Such disordering in ferrocenyl alcohol unsubstituted Cp rings has been seen in other structures deposited to the Cambridge Structural Database, and in the structure of compound **1**, it is likely due to crystal packing effects.^{16(b)} Formation of an intermolecular hydrogen bond from the *meta*-carbon proton of

the cage towards the hydroxyl oxygen (C13...O1) may be attributed to the acidity of the *meta*-carbon proton induced by the electronic deficiency feature of the cage. This intermolecular hydrogen bond links the ferrocenyl hydroxyl group to an infinite one-dimensional chain in the crystal lattice.

Traditional hydrogen bonding interactions (such as O—H...O) are not observed in compound **1** for the hydroxyl H atom, and the absence of such bonding could be attributed to steric and electronic effects. The hydroxyl H atom in compound **1** does engage in intramolecular hydrogen bonding by pointing towards the ferrocenyl Fe atom with an H...Fe distance 3.05 Å and an O...Fe distance 3.533(2) Å. The distance between the hydroxyl H to the closest C atom on the Cp ring is 2.83 Å with an O...C19 distance of 3.62(2) Å in conformation *A*, and 2.81 Å with an O...C19B 3.56(2) Å for conformation *B*. The O...C distance from the hydroxyl O atom towards staggered conformation *A* is greater than that of conformation *B*. Conformation *B* is a better candidate to form a OH... π (Cp)-type hydrogen bond than conformation *A*. Indeed, the eclipsed conformation *B* has a shorter Fe—Cp distance and longer C—C distance, which are closer to those distances seen in a regular ferrocenyl configuration, but still longer. The Fe—Cp distance in the staggered conformation *A* is much longer, and the C—C bond lengths are shorter. One would expect that formation of a OH...Fe hydrogen bond should weaken the Fe—Cp bond, leading to a lengthened Fe—Cp distance. In the structure of compound **1**, the OH... π (Cp) or OH...Fe hydrogen bonds by the hydroxyl H atom with the ferrocenyl group are long and weak.

This interaction between a hydroxyl H atom and the ferrocenyl group is a common feature of many carbinol bridged ferrocenes found in the Cambridge Structural Database.^{1,16(a)–(g)} However, the assignments in the literature of the hydrogen bond involved are far from convincing. Spectroscopic studies^{17(a)–(c)} on the metallocenyl alcohols (Os, Ru and Fe) suggest that there are competing bonding interactions be-

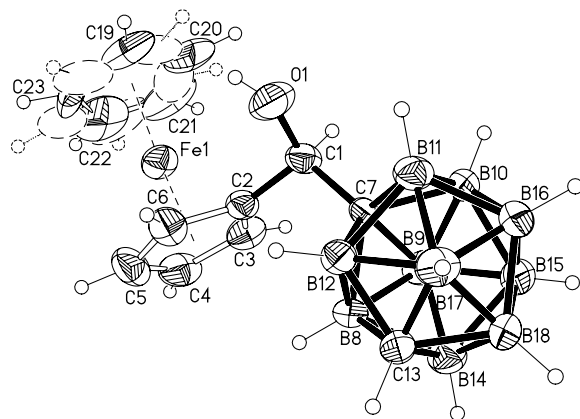


Fig. 2. View of the title compound, showing the atom-numbering scheme and ellipsoids at 50% probability level.

tween the OH... π (Cp) and OH...M hydrogen bonds in the case of Fe. Theoretical calculations for the α -metallocenylcarbinols by Orlova *et al.*¹⁸ support the formation of intramolecular OH...M (M = Os, Ru) hydrogen bonds in their metallocenylCH₂OH model, but their calculation for the ferrocenylCH₂OH model did not find a minimum state corresponding to the formation of an intramolecular OH...Fe hydrogen bond. Furthermore, their model did not consider the probable OH... π (Cp) interaction. Computational chemistry calculations with a careful selection of basis sets and inclusion of the electronic effect due to the methylene group with a ferrocenylCHROH model may provide insights into this interaction (Figs. 2 and 3).

Conclusion

The reaction of *m*-carborane with TBAF and *n*-BuLi produces highly reactive species susceptible to electrophilic attack. The mono-substituted product is preferentially obtained since the formation of di-substituted products is hindered, due to a decrease in the nucleophilicity of the unsubstituted carborane carbon following substitution of the other carbon atom. Instability observed in **1** is likely the result of localized

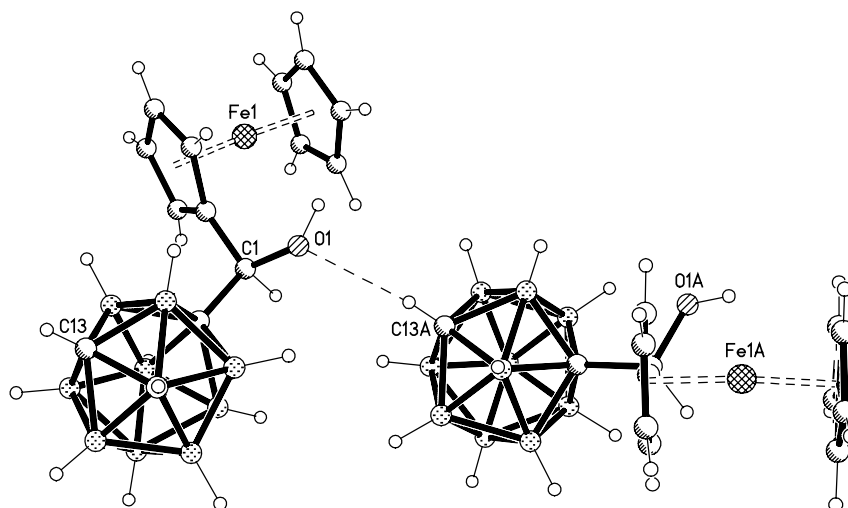


Fig. 3. Balls and Sticks plot of compound **1** showing the intermolecular hydrogen bond from the *meta*-carbon H of the carborane towards the hydroxyl oxygen.

electronic networks on the carborane and ferrocene subunits separated by the carbinol linker, as a result there appears to be a tendency for the carborane and ferrocene subunits to separate at the methyl hydroxy bridge. Based on crystallographic data, the carbinol bridge is held more closely to the ferrocene subunit, C1–C2 bond length = 1.498(4) Å versus C1–C7 bond length, 1.560(4) Å. A system where the electronic network is delocalized throughout the carborane linkage and ferrocene units would likely result in a more stable complex. Further work in developing novel carboranyl species with ferrocenyl moieties is in progress.

Acknowledgments

The authors gratefully acknowledge financial support for this research by grants from the National Science Foundation (CHE-0136724, DMR-0351848, and CHE-0515363), and the National Institutes of Health (R15 AI055515-01). The Center for Molecular Structure has been supported by the W.M. Keck Foundation and the California State University Program for Education and Research in Biotechnology.

References

1. Arellanes, C.; Gomez, F.A.; Crundwell, G.; Kantardjieff, K. *Acta Cryst.* **1998**, *C54*, IUC9900087.
2. Hermansson, K.; Wójcik, M.; Sjöberg, S. *Inorg. Chem.* **1999**, *38*, 6039.
3. Nakamura, H.; Aoyagi, K.; Yamamoto, Y. *J. Amer. Chem. Soc.* **1998**, *120*, 1167.
4. Gomez, F.A.; Hawthorne, M.F. *J. Amer. Chem. Soc.* **1992**, *57*, 1384.
5. Grimes, R. N. *Carboranes*; Academic: New York, 1970.
6. Siebert, W. *Advances in Boron Chemistry*; The Royal Society of Chemistry: Cambridge, UK, 1997.
7. Hawthorne, M. F.; Maderna, A.; Grafstein, D. *Chem. Rev.* **1999**, *99*, 3421.
8. Wong, W.; Lu, G.; Choi, K.; Guo, Y. *J. Organomet. Chem.* **2005**, *99*, 3421.
9. Tsuboya, N.; Lamrani, M.; Hamasaki, R.; Ito, M.; Mitsuishi, M.; Miyashita, T.; Yamamoto, Y. *J. Mater. Chem.* **2002**, *12*, 2701.
10. Schleyer, P. von R.; Najafian, K. in “*The Borane, Carborane, Carbocation Continuum*”, edit. J. Casanova, John Wiley and Sons, New York, 1998.
11. Spartan '02 for Linux/Unix, Wavefunction, Inc., Irvine, CA.
12. SMART, Software for the CCD Detector System, version 5.05 (NT); Bruker Analytical X-ray Systems: Madison, WI, 1998.
13. SAINT, Software for the CCD Detector System, version 5.01 (NT); Bruker Analytical X-ray Systems: Madison, WI, 1998.
14. Blessing, R.H. SADABS, Program for Absorption Corrections Using Siemens CCD Based on the Method of Robert Blessing; *Acta Crystallogr.* **1995**, *A51*, 33–38.
15. (a) Sheldrick, G.M. SHELXS-90, Program for the Solution of Crystal Structure; University of Göttingen: Germany, 1990. (b) Sheldrick, G.M. SHELXL-97, Program for the Refinement of Crystal Structure; University of Göttingen: Germany, 1997. (c) SHELXTL 5.10, Program Library for Structure Solution and Molecular Graphics, PC Version; Bruker Analytical X-ray Systems: Madison, WI, 1998.

16. (a) Dimitrov, V.; Linden, A.; Hesse, M. *Tetrahedron: Asymm.* **2001**, *12*, 1331. (b) Ferguson, G.; Gallagher, J. F.; Glidewell, C.; Zakaria, C. M. *Acta Crystallogr., Sect. C: Cryst. Struct. Commun.* **1993**, *49*, 967. (c) Routaboul, L.; Chiffre, J.; Balavoine, G.G. A.; Daran, J.-C.; Manoury, E. *J. Organomet.Chem.* **2001**, *637*, 364. (d) Glidewell, C.; Klar, R. B.; Lightfoot, P.; Zakaria, C. M.; Ferguson, G. *Acta Crystallogr., Sect. B: Struct. Sci.* **1996**, *52*, 110. (e) Troitskaya, L. L.; Demeshchik, T. V.; Ovseenko, S. T.; Starikova, Z.A.; Sokolov, V. I.; Malezieux, B.; Gruselle, M. *Izv. Akad. Nauk SSSR, Ser. Khim. (Russ.) (Russ. Chem. Bull.)* **2003**, 591. (f) Skibar, W.; Kopacka, H.; Wurst, K.; Salzmann, C.; Ongania, K.-H.; de Biani, F.F.; Zanello, P.; Bildstein, B. *Organometallics* **2004**, *23*, 1024. (g) Bryce, M.R.; Skabara, P. J.; Moore, A.J.; Batsanov, A. S.; Howard, J.A.K.; Hoy, V.J. *Tetrahedron* **1997**, *53*, 17781.
17. (a) Trifan, D.S.; Weinmann, J.F.; Kuhn, L.P. *J. Am. Chem. Soc.* **1957**, *79*, 6567. (b) Shubina, E.S.; Epstein, L. M.; Timofeeva, T.V.; Struchkov, Yu.T.; Kreindlin, A.Z.; Fadeeva, S.S.; Rybinskaya, M.I. *J. Organomet. Chem.* **1991**, *401*, 133. (c) Shubina, E.S.; Epstein, L.M.; Kreindlin, A.Z.; Fadeeva, S.S.; Rybinskaya, M.I. *J. Organomet. Chem.* **1991**, *401*, 145.
18. Orlova, G.; Scheiner, S. *Organometallics*, **1998**, *17*, 4362.